

Supplementary Information

Ultra-small MgH_2 nanoparticles embedded into an ordered microporous carbon with rapid hydrogen sorption kinetics

by Claudia Zlotea ^a, Yassine Oumellal ^a, Son-Jong Hwang ^b, Camelia Ghimbeu Matei ^c, Petra de Jongh ^d, Michel Latroche ^a

Content:

- 1) Pore size distribution of pristine carbon template CT
- 2) Hydrogenation of $\text{MgBu}_2@CT$ followed by HP-DSC
- 3) N_2 sorption measurement at 77 K for all $\text{MgH}_2@CT$ composites before and after HCl leaching
- 4) X-rays diffraction for pristine CT carbon and $50\text{MgH}_2@CT$ composite after leaching
- 5) Comparative study for determination of the activation energy of desorption of bulk MgH_2
- 6) ^1H MAS NMR spectra from the CT and $15\text{MgH}_2@CT$ and related deconvolutions

1) Pore size distribution of pristine ordered microporous carbone CT

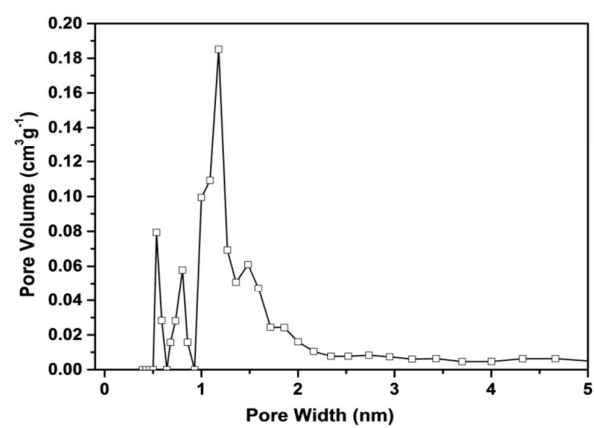


Figure SI-1. Pore size distribution of pristine carbon template CT from zeolite β .

2) Hydrogenation of $\text{MgBu}_2@\text{CT}$ followed by HP-DSC

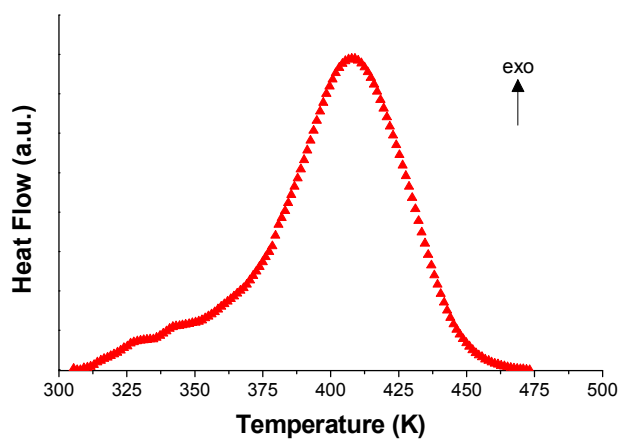


Figure SI-2. HP-DSC curve during hydrogenation reaction: $\text{Bu}_2\text{Mg}@\text{CT} + \text{H}_2 \rightarrow \text{MgH}_2@\text{CT} + 2\text{C}_4\text{H}_{10}\uparrow$ under 2.5 MPa H_2 with a constant heating rate of $5 \text{ K}\cdot\text{min}^{-1}$.

3) N_2 sorption measurement at 77 K for all $MgH_2@CT$ composites before (as-synthesized) and after HCl leaching

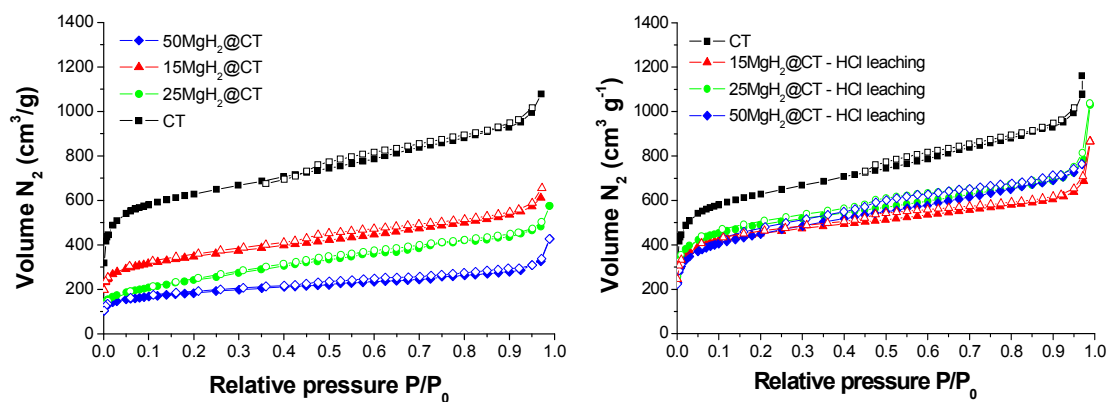


Figure SI-3. N_2 sorption isotherms at 77 K for all $MgH_2@CT$ composites as synthesized (left) and after HCl leaching (right).

4) X-rays diffraction for the pristine CT carbon and the 50MgH₂@CT composite after leaching

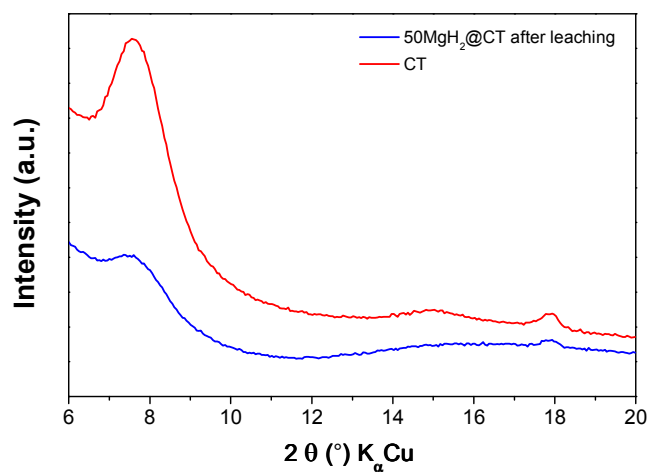


Figure SI-4. X-rays diffraction of the pristine CT and the composite 50MgH₂@CT after leaching.

The X-rays diffractometer used is described in the experimental section. The diffraction peak at 7.5 ° strongly decreases after acid leaching of 50MgH₂@CT as compared to the pristine CT. This indicates a loss of structural ordering by insertion of MgH₂ nanoparticles, in agreement with previous results. [1]

5) Comparative study for the determination of activation energy of desorption of bulk MgH_2

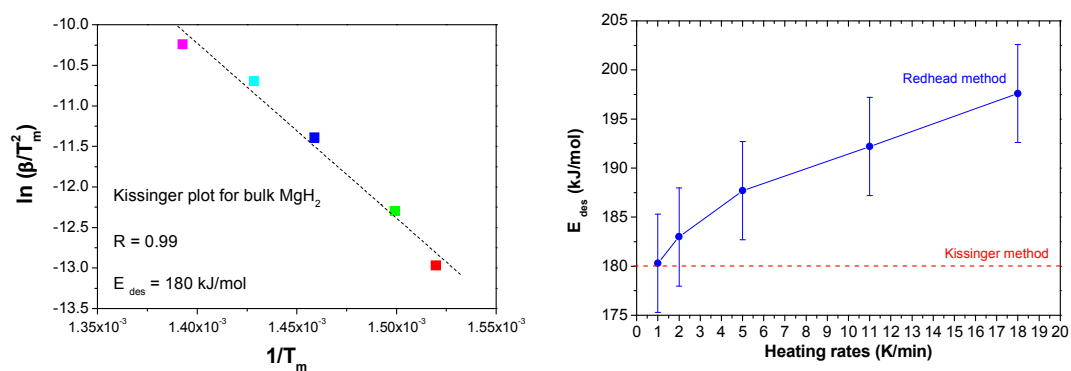


Figure SI-5. Kissinger plot for bulk MgH_2 (left) and the comparison between the activation energies of desorption as calculated from Kissinger and Redhead methods (right).

The E_{des} value calculated by Redhead method [2] for the slowest heating rate ($1 \text{ K} \cdot \text{min}^{-1}$) matches the one determined by Kissinger method suggesting that Redhead equation gives accurate results from our spectra recorded with low heating rates ($1\text{-}2 \text{ K} \cdot \text{min}^{-1}$).

6) ^1H MAS NMR spectra from the CT, $15\text{MgH}_2@\text{CT}$ and $50\text{MgH}_2@\text{CT}$ and related deconvolution for $15\text{MgH}_2@\text{CT}$

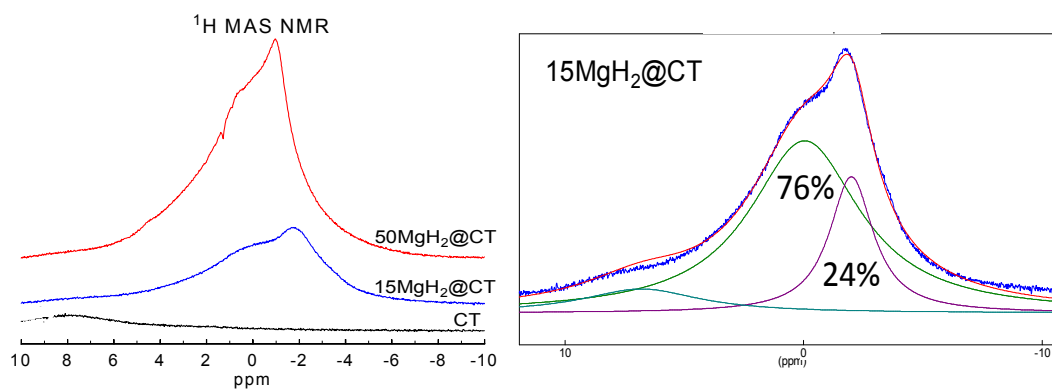


Figure SI-6. ^1H MAS NMR spectra from the CT, $15\text{MgH}_2@\text{CT}$ and $50\text{MgH}_2@\text{CT}$ (left) and related deconvolution for $15\text{MgH}_2@\text{CT}$ (right).

References:

- [1] C. M. Ghimbeu, C. Zlotea, R. Gadiou, F. Cuevas, E. Leroy, M. Latroche, and C. Vix-Guterl, *J. Mater. Chem.* **21**, 17765 (2011).
- [2] A. Dejong and J. Niemantsverdriet, *Surf. Sci.* **233**, 355 (1990).